# Surfactant-Induced Ordering and Wetting Transitions of Droplets of Thermotropic Liquid Crystals "Caged" Inside Partially-Filled Polymeric Capsules

*Rebecca J. Carlton, Yashira M. Zayas-Gonzalez, Uttam Manna, David M. Lynn,* and Nicholas L. Abbott**

Department of Chemical and Biological Engineering, University of Wisconsin – Madison, 1415 Engineering Drive, Madison, WI 53706 (USA)

***Supporting Information***

**Materials.** Spherical monodisperse silica ($SiO_2$) particles with a diameter of 4.99 ± 0.22 μm were purchased as an aqueous suspension (5% w/v) from Microparticles GmbH (Berlin, Germany). Branched poly(ethyleneimine) (PEI, $M_W$ ~ 25,000), tetrahydrofuran (THF), DMSO, 2,2′-azoisobutyronitrile (AIBN), 1-aminodecane (*n*-decylamine, DA), and acetone were purchased from Sigma-Aldrich (Milwaukee, WI). Sodium dodecyl sulfate (SDS) was obtained from Aldrich Chemical Company, Inc., (Milwaukee, WI), and dodecyltrimethylammonium bromide (DTAB) was obtained from Sigma-Aldrich Co., (St. Louis, MO). 6-Aminofluorescein (FL) was purchased from TCI America (Portland, OR). 3-Dimethylaminopropylamine (99%)

was purchased from Acros Organics (New Jersey, USA). 2-Vinyl-4,4-dimethylazlactone (VDMA) was a gift from Dr. Steven M. Heilmann (3M Corporation, Minneapolis, MN). Poly(2-vinyl-4,4-dimethylazlactone) (PVDMA, $M_W$ ~ 10,300; dispersity, D = 3.2) was synthesized by free-radical polymerization of VDMA according to previously published methods.[17] PVDMA labeled with FL (2 mol%; $PVDMA_{FL}$) was synthesized according to published methods.[17] J.T. Baker Buffered Oxide Etch (BOE), 10:1, containing water, ammonium fluoride, and hydrogen fluoride (HF) was obtained from Mallinckrodt Baker, Inc. (Phillipsburg, NJ). Ethanol was purchased from Decon Laboratories, Inc. (King of Prussia, PA). E7 (a mixture of cyanobiphenyl-containing nematogens) was purchased from EMD Chemicals (Philadelphia, PA). A Milli-Q system (Millipore, Bedford, MA) was used to produce water with a resistivity of 18.2 MΩ·cm. Fisher's Finest Premium Grade microscope cover glasses were obtained from Fisher Scientific (Pittsburgh, PA). Eppendorf microcentrifuge tubes were purchased from Axygen, Inc. (Union City, CA).

*Layer-by-layer fabrication of polymer multilayers on silica microparticles:*

The first layer of PEI was deposited onto the $SiO_2$ microparticles by adding 1 mL of the PEI solution to the particles and manually shaking the microparticles for 1 min to allow sufficient time for the polymer to adsorb to the particle surface. The microparticles were then centrifuged for 2 min at 1500 rpm. The supernatant was carefully removed by pipette, and the microparticles were rinsed two times by resuspending them in 1 mL of acetone and vortexing. After each rinse in acetone, the microparticles were centrifuged for 2 min at 1500 rpm and the supernatant was removed. The second layer of the multilayered film was then deposited by adding 1 mL of PVDMA solution (either PVDMA or $PVDMA_{FL}$, as necessary) to the particle

suspension and shaking manually for 30 s with brief sonication to allow sufficient time for the PVDMA to react with primary amines in the previously deposited PEI layer. The microparticles were then rinsed two times with 1 mL of acetone as described above. Subsequent layers were fabricated by repeating this process (by alternately depositing PEI or PVDMA solutions and allowing each layer to react for 30 s) until the desired number of polymer PEI/PVDMA layer pairs (or 'bilayers') were deposited onto the particle surface.

*Characterization of functionalized capsules:*

As described in the main text, we chose to create capsules having hydrophobic interior functionality (DA) and hydrophilic exterior functionality (DM) through a two-step dual-functionalization procedure (see **Figure 1B** in the main text and surrounding discussion). To demonstrate proof of concept and verify that this two-step approach could be used to create capsules possessing one functional group covalently attached to the inner layers of the capsule and a second functional group attached to the outer layers of the capsule, we prepared capsules for which the first two bilayers were reacted with tetramethylrhodamine (TMR-$NH_2$) and the second two bilayers, added subsequent to functionalization with TMR-$NH_2$, were functionalized with fluorescein-$NH_2$. Fluorescence microscopy confirmed the incorporation of both fluorophores in the capsules (as shown in **Figure S1** below). However, the optical resolution of the fluorescence from the functionalized capsules did not allow us to determine if the fluorophores were spatially separated into inner and outer functionalities, but rather they appeared to be co-localized at the resolution used. We note that during imaging, some capsules were mobile and moved between the capture of images for both the red and green channels. We

selected a subset of capsules that had settled on the glass coverslip prior to imaging as a representative region (**Figure S1** below).

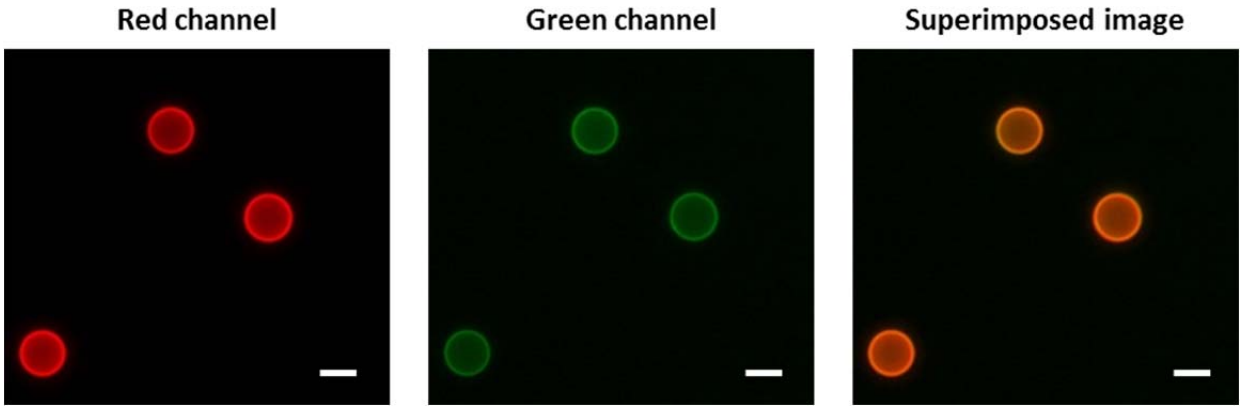


**Figure S1**. Representative fluorescence micrographs of hollow capsules. TMR, fluorescein, and superimposed channels are displayed from left to right. Co-localization of fluorescence signals of capsules that had settled onto the glass slide demonstrates incorporation of two functional motifs into the polymeric microcapsules. Scale bars are 5 μm.

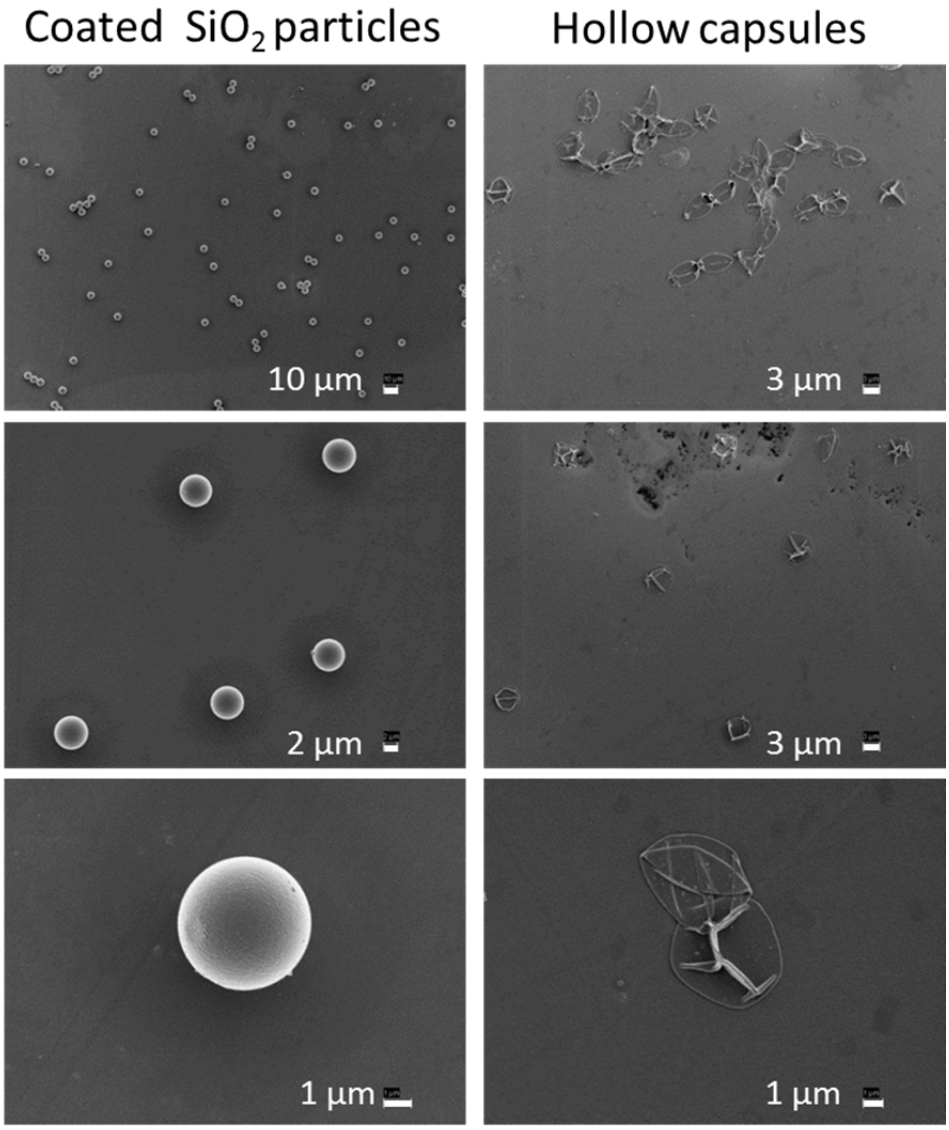


**Figure S2**: SEM images of dried, polymer-coated microparticles and hollow capsules. Samples were dried and coated with a thin layer of gold using a sputterer prior to imaging. From the images of the coated particles, the size was measured to be 4.86 ± 0.2 µm. Inspection of the SEM images of the hollow capsules reveals that they are flexible and collapse upon drying.

*Contact angle histograms*:

As mentioned in the main text, we observed a subpopulation of distorted, non-spherical LC droplets (see **Figure 4D**). This population is also evident from measurements of contact angles of the LC droplets on the inner capsule walls as shown in the histograms plotted in **Figure S3**, below. Specifically, for caged LC droplets in water (blue bars), there are two peaks on the histogram of the contact angle. However, when caged droplets from this same batch preparation were added to a 10 mM DTAB solution (**Figure S3A**, red bars), the average contact angle increased slightly, and there was only one peak in the histogram. This suggests that DTAB releases the forces that pin the contact line of the distorted LC droplets. Inspection of **Figure S3B** reveals the heterogeneity of droplet shapes that exists as SDS is added, resulting in a majority of droplets possessing a hemispherical shape (average contact angle ~90°) in 0.25 mM SDS (orange bars). See also **Figure 6** in the main text for the average contact angle values.

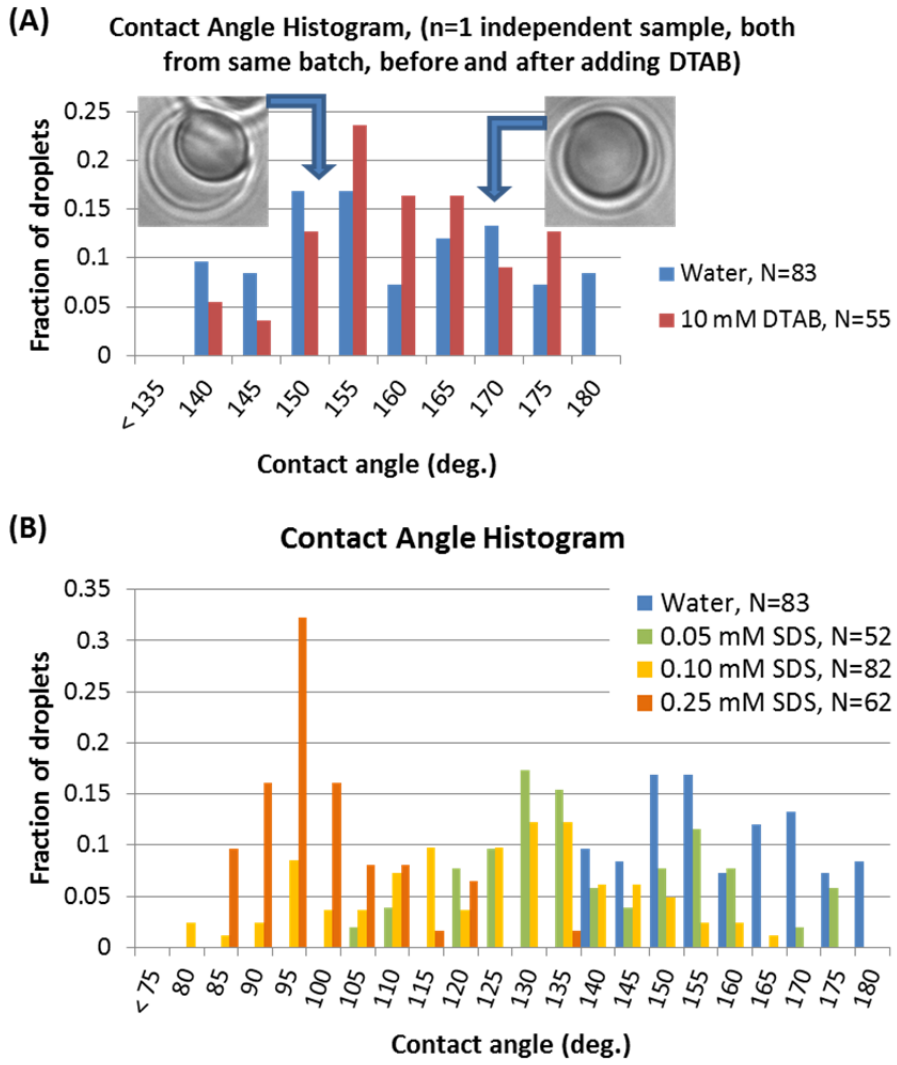


**Figure S3**: Histograms of the contact angles measured for caged LC droplets in water or surfactant solutions. (A) Comparison of histograms for droplets in water or 10 mM DTAB. Only one independent sample preparation is shown, providing a before-and-after of the effect of adding DTAB. Inset images from Figure 4 in the main text are shown for droplets in water with arrows indicating which peak in the histogram they represent. (B) Comparison of the histograms for water or 0.05 mM, 0.10 mM, or 0.25 mM SDS. All x-axis values represent the upper limit of a bin, e.g. the label "180" corresponds to a bin in the histogram for values of the contact angle in the range of 175-180.

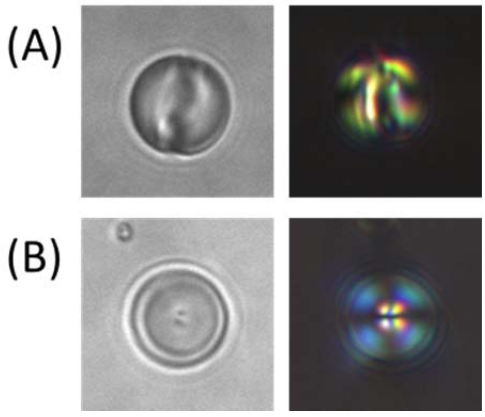


**Figure S4**: Brightfield and polarized light micrographs of bare LC droplets contacted with varying concentrations of DTAB. (A) In 2 mM DTAB, an E7 droplet with a diameter of 7.3 μm appears in a Saturn-ring configuration. (B) In 10 mM DTAB, an E7 droplet with a diameter of 7.4 μm appears in a radial ordering configuration.

*Details regarding the SI video of encapsulated LC droplets in 1 mM SDS:*

A video has also been included in the online SI (found at http://pubs.acs.org). The video is composed of an image sequence, captured at one frame per second, of "caged" LC droplets in 1 mM SDS. As the caged droplets rotate and translate across the field of view, the analyzer was inserted and removed to show both brightfield and crossed polarized light views. Most of these droplets exhibit a concave-hemisphere shape with ordering that is topologically equivalent to spherical radial droplets. At ~10s, a droplet with ordering topologically equivalent to the axial or Saturn-ring configuration enters the top right of the field of view; in the frames between ~12-15 s, the side and top views of the droplet are apparent as it rotates. (See **Figure 8** in the main text.)